Available online at www.sciencedirect.com
ScienceDirect
Materials Chemistry and Physics 110 (2008) 186–191
MATERIALS CHEMISTRY AND PHYSICS
www.elsevier.com/locate/matchemphys

Hydrothermal synthesis of $BaTiO_3$: Crystal phase and the Ba^{2+} ions leaching behavior in aqueous medium

Changlong Chen [a,c,*], Yuling Wei [b], Xiuling Jiao [c], Dairong Chen [c]

[a] School of Chemistry and Chemical Engineering, University of Jinan, Jinan 250022, PR China
[b] Department of Science and Technology, Shandong Institute of Light Industry, Jinan 250353, PR China
[c] School of Chemistry and Chemical Engineering, Shandong University, Jinan 250100, PR China

Received 18 September 2007; received in revised form 18 January 2008; accepted 25 January 2008

Abstract

Continuous phase transition from cubic-to-tetragonal depended on reaction conditions was found in the hydrothermally synthesized $BaTiO_3$. The $BaTiO_3$ particles were characterized by powder X-ray diffraction (XRD), transmission electron microscope (TEM), high resolution TEM (HR-TEM), Raman spectra and thermal gravimetric analysis (TGA) techniques. A competitive process between the kinetic control and the thermodynamic control resulted in the crystal structure transition. In these structure-transitional products, the "cubic-rich" $BaTiO_3$ exhibited a stronger Ba^{2+} ions leaching ability in aqueous medium compared with the "tetragonal-rich" $BaTiO_3$ because the two types of samples had differences in crystal structures and the amount of lattice defects contained.

Keywords: Electronic materials; Hydrothermal synthesis; Phase transitions; $BaTiO_3$

1. Introduction

Barium titanate ($BaTiO_3$) is an important electro-ceramic material that is widely used in fabrication of multilayer ceramic capacitors (MLCCs), communication filters, positive temperature coefficient of resistivity (PTCR) thermistors and sensors [1–4]. The conventional synthetic methods for $BaTiO_3$ mainly include solid-state reaction [5], sol–gel technique [6–8], co-precipitation [9], and microwave heating [10]. Hydrothermal method, because of its outstanding advantages such as mild reaction conditions, pure products with a narrow size distribution, low particle agglomeration and high reactivity during sintering, is another synthetic approach that has been widely used to prepare $BaTiO_3$ for the last decades [11–18]. As known, $BaTiO_3$ exists in different crystalline structures, of which the most studied are cubic and tetragonal polymorphs. It was reported that the transition from the ferroelectric tetragonal polymorphic form to the paraelectric cubic one, occurred at the Curie point of *ca.* 130 °C [19,20], could be affected markedly by the particle size especially when it is sufficiently small [21–24]. Synthesis temperatures can also affect the crystal structure. Busca et al. pointed out that the hydrothermally synthesized $BaTiO_3$ (at 358 K for 6 h) showed the XRD pattern of cubic structure but a Raman spectrum associated with a lower symmetry [20]. Burtrand I. Lee found that the $BaTiO_3$ synthesized hydrothermally at 230 °C for 0.5–2 h showed a cubic structure with some tetragonality [22]. Other factors, for example, starting materials, that have influences on the crystal structure of $BaTiO_3$ was also reported [14–16]. Although the crystalline $BaTiO_3$ obtained by hydrothermal method have been investigated so extensively, disputes still exist. For instance, does the cubic $BaTiO_3$ really exists at room temperature or in fact it is a natural tetragonal structure merely with a *c*/*a* value very close to one [22,24]. However, to our best knowledge, such debates rarely focused on the cubic-to-tetragonal transition mechanism of $BaTiO_3$ in hydrothermal process. Because the change of $BaTiO_3$ phase structure itself is a subject of thermodynamics, the parameters affecting the thermal equilibrium should be much considered.

On the other hand, $BaTiO_3$ is not thermodynamically stable in aqueous solution because barium ions (Ba^{2+}) will leach from the particle surface, which results in the formation of a titanium-rich

* Corresponding author at: School of Chemistry and Chemical Engineering, University of Jinan, Jiwei Road 106, Jinan 250022, PR China.
Tel.: +86 531 82289601; fax: +86 531 89631632.
E-mail address: ccl@mail.sdu.edu.cn (C. Chen).

0254-0584/$ – see front matter © 2008 Elsevier B.V. All rights reserved.
doi:10.1016/j.matchemphys.2008.01.031

outer layer [25,26–28], shown in the following reaction:

$$BaTiO_3(s) + H_2O = Ba^{2+}(aq) + TiO_2(s) + 2OH^-(aq) \quad (1)$$

The leaching of Ba^{2+} ions causes the deviation in stoichiometry of $BaTiO_3$. This result will affect the quality of the fabricated ceramic devices derived from $BaTiO_3$, and then cause the degradation of their dielectric properties [2]. Consequently, the leaching of Ba^{2+} ions from $BaTiO_3$ in aqueous system is a major issue in the field of fabrication of $BaTiO_3$-based electroceramics [25,29]. Early investigations focused mainly on the influences of different parameters, such as pH values, solids concentrations, $BaCO_3$ impurity and the polyelectrolytes addition, on the $BaTiO_3$ stability in aqueous suspensions [2,30–33]. However, effects of $BaTiO_3$ phase structures on the Ba^{2+} ions leaching behavior rarely reported.

In this work, we report the hydrothermal synthesis of $BaTiO_3$ and their continuous phase transition from cubic-to-tetragonal based on the reaction condition changing. The effects of the phase structure on Ba^{2+} ions leaching behavior of the $BaTiO_3$ ceramic particles in the aqueous suspensions are discussed as well.

2. Experimental

2.1. Synthesis

All materials used in present experiments are analytical grade. 3.3 mL (30 mmol) $TiCl_4$ was diluted by 7.0 mL hydrochloric acid (2.0 mol dm^{-3}) to form a yellowish solution, and 7.3 g $BaCl_2{\cdot}2H_2O$ was dissolved in 30 mL deionized water. The two solutions were mixed to form barium titanium solution. Under stirring and N_2 bubbling, 40 mL NaOH aqueous solution (6.0 mol dm^{-3}) was added to the barium titanium solution and a white homogeneous colloidal barium titanium slurry was formed. Afterward, 12 mL barium titanium slurry was poured into a stainless steel autoclave lined with Teflon with a capacity of 15 mL. The autoclave was heat-treated at predetermined temperature for a certain time. After cooled to room temperature, the supernatant in the autoclave was poured out and the white precipitation was filtrated and washed with deionized water for six times. Lastly, the products were obtained after drying at 80 °C for 5 h.

2.2. Characterization

The XRD data were recorded on a Rigaku D/MAX 2200 PC X-ray diffractometer using Cu Kα radiation (λ = 0.15418 nm) and a graphite monochromator at ambient temperature. The unit cell parameters of the particles were calculated via the refinement program of Jade 5.0 matched to the X-ray diffractometer using the data of the following six diffraction planes: (1 0 0), (1 1 0), (1 1 1), (2 0 0), (2 1 0) and (2 1 1). During the experiments, KCl crystals were employed as an internal standard material. The products were characterized using TEM and HRTEM (Philips Tecnai 20U-TWTN) operating at 200 kV. The specific surface area of the particles was characterized with Surface Area & Pore Size Analyzer (NOVA 2000e). The Raman spectra were recorded using a Jasco Ventuno[21] Micro Raman Spectrophotometer with laser (532 nm) power of 30 mW. The element analysis was performed on an inductively couple plasma atomic emission spectrometer (ICP-AES) (PE Instruments ICP-OES Optima 2000 DV) at ambient temperature.

2.3. Measurement of the Ba^{2+} ions leaching

In a typical experiment, 20 mg powder was added into 1.25 mL hydrochloric acid (pH 2) in a plastic tube. The sealed plastic tube was ultrasonic treated for 5 min with a power of 120 W and then was equilibrated at room temperature for 4 h. After that, the suspension was centrifuged at a speed of 9500 rpm for 30 min. The Ba^{2+} ions in the supernatant were measured by ICP-AES at ambient temperature.

3. Results and discussion

3.1. Synthesis of $BaTiO_3$ and the particulate properties

Fig. 1 shows the XRD patterns of the samples obtained at different hydrothermal conditions, exhibiting that all the products are of good crystallization. Increasing reaction temperatures, as shown in Fig. 1, bottom, the diffraction peaks of different samples reveal various degrees of shift to higher angles and only the 120 °C-product (pattern a) does fit well with the typical reflection of cubic $BaTiO_3$ (JCPDS, No.31-0174). Such peak-shift is negligible at low angles, for example, {1 0 0} planes, however, it becomes more distinct at higher angles. It is obvious that the reaction temperature has a remarkable effect on the crystal structure, i.e. increasing reaction temperatures will cause contin-

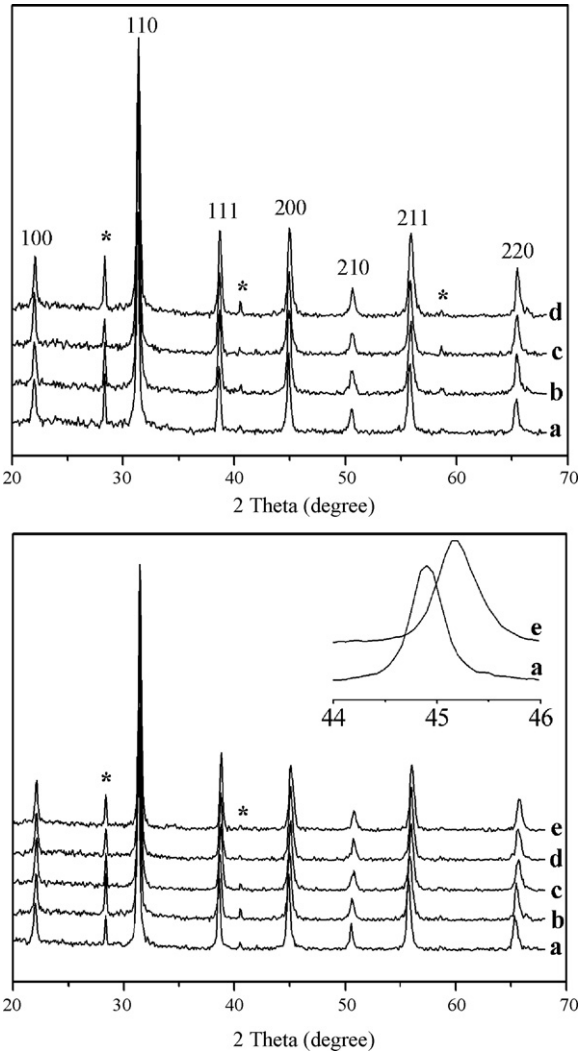

Fig. 1. XRD patterns of the samples hydrothermally synthesized at different conditions. Bottom: 4 h and (a) 120 °C, (b) 140 °C, (c) 160 °C, (d) 180 °C and (e) 200 °C. Top: 140 °C and (a) 1 h, (b) 2 h, (c) 3 h and (d) 4 h. Asterisk (*) indicates the peak of the internal standard material (KCl).

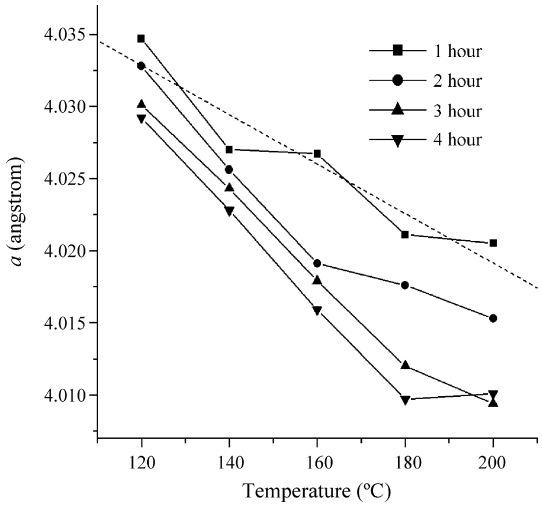

Fig. 2. The values of the lattice constant a of the hydrothermally synthesized $BaTiO_3$ as a function of the reaction temperatures with different reaction time.

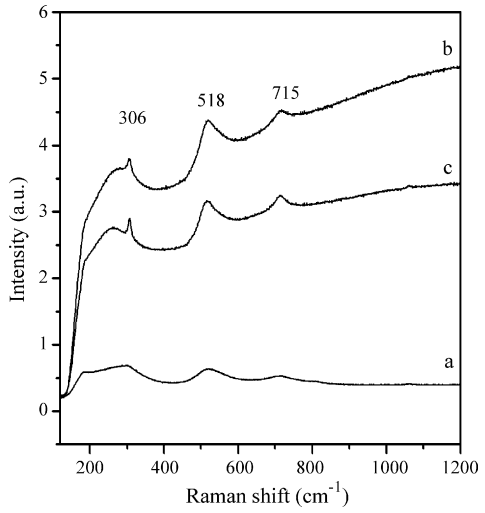

Fig. 3. Raman spectra of $BaTiO_3$ particles synthesized at (a) 120 °C/1 h, (b) 160 °C/4 h and (c) 200 °C/4 h.

uous crystal cell variation. Such effects can be exhibited by the position changing of {2 2 0} reflection planes. When the reaction temperature increases from 120 °C to 200 °C, the {2 2 0} peak shifts from $2\theta = 55.696°$ to $2\theta = 56.011°$. In fact, the peaks of the 200 °C-product (pattern e) have so big shifts that they nearly overlap those of the tetragonal $BaTiO_3$ (JCPDS No.5-0626), although the diffraction peak of {2 0 0} plane do not split (Fig. 1, bottom, inset). In addition, the effect of reaction time on the cell variation is also investigated. As shown in Fig. 1, top, prolonging reaction time also causes the diffraction peaks shifting to high angles, although the peak shifts are not as obvious as those caused by raising reaction temperature. To exhibiting this lattice variation more clearly, cell constants of the different samples are calculated using their diffraction data. Herein, because the XRD patterns reveal the characteristics of cubic $BaTiO_3$ without certain peak splitting, the variation of constant a is investigated. As shown in Fig. 2, the parameter is clearly decrescent when the reaction conditions vary from low temperature/short time to high temperature/long time. Moreover, this trend becomes nearly linearization when the reaction time is longer than 2 h at 120–180 °C. However, the decreasing of cell constant ceases when the reaction temperature gets to 200 °C and reaction time gets to 4 h, where the smallest a of *ca.* 4.010 Å is obtained.

Fig. 3 shows the Raman spectra of $BaTiO_3$ samples obtained at different reaction conditions. As shown, curves b and c reveal obvious Raman-active modes for tetragonal $BaTiO_3$ [16,20]. The peak at 518 cm^{-1} is assigned to the TO mode of A_1 symmetry, and the sharp peak at 306 cm^{-1} is attributed to the B_1 mode, which is the characteristics of tetragonal $BaTiO_3$ [20,21,34]. The weak peak at 715 cm^{-1} is assigned to the highest-frequency longitudinal optical mode (LO) with A_1 symmetry. In contrast, these active modes attributed to tetragonal $BaTiO_3$ do not clearly appear on curve a, in which only weak plasmon peaks were shown, indicating that the tetragonality of the crystal is much less. Such characteristics confirm the transition of $BaTiO_3$ from cubic to tetragonal with the increasing of reaction temperature and/or prolonging of reaction time, which agrees well with the results showed in the XRD patterns.

It is well known that $BaTiO_3$ undergoes a transition from the cubic phase (space group $Pm3m = O_h$) to tetragonal one (space group $P4mm = C_{4v}$) around the Curie point (130 °C) with small shifts of titanium and oxygen ions along the c direction toward opposite sides, and becomes thermodynamically stable at room temperature [20,22]. From the XRD results it can be seen that the tetragonality of hydrothermal $BaTiO_3$ is affected by reaction temperature as well as reaction time. The changing of $BaTiO_3$ cell parameters based on the variation of hydrothermal reaction conditions is attributed to the energy-minimizing tendency of the system. The crystallization of $BaTiO_3$ is dominated by kinetics at low temperature and in short reaction time, but a thermal equilibrium will play a key role at higher temperature and/or in a long reaction time. It is in the kinetics-control stage that the metastable cubic $BaTiO_3$ crystallize. In this stage, lots of lattice defects are formed in the form of OH^- ions and their compensation of cation cavities [22,23,35]. When the reaction proceeds at higher temperature and/or for a long time, the thermodynamic control will play a dominant role. This thermodynamic equilibrium results in minimizing of the crystal energy and formation of stable structures by reducing the point defects in the crystals. In this situation, distortion of TiO_6 octahedron occurs for the purpose of reducing energy and cubic $BaTiO_3$ possessing some tetragonality forms. But such distortion is very small when the reaction conditions are mild, and c/a value is still close to 1, resulting in the pseudo-cubic structure shown in the XRD patterns. Even for the sample obtained at 200 °C, whose XRD diffraction peaks nearly overlap the reflections of tetragonal $BaTiO_3$, peak splitting does not appear. Particularly, the competition between the kinetics-control process and the thermodynamics-control process can be illustrated clearly by the samples obtained after hydrothermal treatment for 1 h. As shown in Fig. 2, after linear fitting, curve a (1 h) has a slope slower than those of the other three curves. It indicates that at the initial 1 h the tetragonality of the product is not the domi-

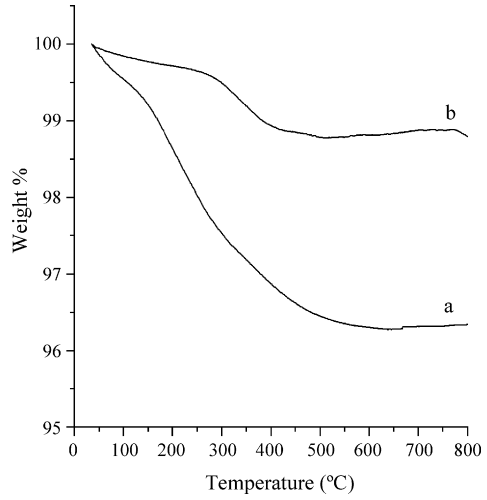

Fig. 4. TG analyses of $BaTiO_3$ particles synthesized at (a) 120 °C/1 h and (b) 200 °C/4 h.

nant, even at a reaction temperature of 200 °C. If the reaction time is longer than 1 h, as shown, the cell constants nearly linearly descend with the reaction temperatures increasing. It can be concluded that the certain reaction conditions provides a certain equilibrium point at which the competition between kinetics and thermodynamics decides the structure of the hydrothermal $BaTiO_3$ crystal.

The existence of lattice defects in the as-synthesized $BaTiO_3$ crystal is also analyzed by TG technique. Fig. 4 shows TGA curves of two distinct samples. The 120 °C-product with a reaction time of 1 h (Fig. 4, curve a) demonstrates a weight loss of *ca.* 3.7% at 50–600 °C whereas the 200 °C-product with a reaction time of 4 h (Fig. 4, curve b) reveals only a weight loss of *ca.* 1.2% at 270–500 °C. Due to the samples are pretreated under vacuum for 24 h, the presence of adsorbed water can be excluded. It should attribute this weight loss to the lattice defects, such as OH^- ions. It is obvious that the sample with big lattice constant *a*, i.e. the "cubic-rich" $BaTiO_3$, contains more amount of OH^- ions than that of the "tetragonal-rich" $BaTiO_3$.

The morphology and the microstructure characteristics of the as-synthesized $BaTiO_3$ particles are characterized with TEM and HRTEM. As shown in Fig. 5a and d, the TEM images with low-magnification reveal that the particles are nearly spherical and have a size of 50 ± 20 nm. These bright-field TEM images also show that a lot of strains are existed in the cubic-rich $BaTiO_3$ particles (Fig. 5a), whereas, the tetragonal-rich $BaTiO_3$ particles (Fig. 5d) are uniform in contrast. $BaTiO_3$ particles, especially the cubic-rich $BaTiO_3$, synthesized via wet chemical methods were verified containing structural defects, mainly in form of lattice OH^- ions and cation vacancies, which results in the particle strains [22,23,35,36]. HRTEM images of the synthesized $BaTiO_3$ particles give more clear observation of the microstructures of the $BaTiO_3$ particles. As can be seen, the lattice fringes of the 120 °C/4 h-product are inhomogeneous in the whole particle (Fig. 5b). The HRTEM image obtained at higher magnification shows clear structure defects (denoted as the white circles in Fig. 5c). On the contrary, as shown in Fig. 5e, the 200 °C/4 h-product reveals a very homogenous lattice fringe phase. The shown lattice plane distance of *ca.* 0.282 nm is indexed to the (1 1 0) planes. The other two groups of crystal planes with same lattice plane distance of *ca.* 0.286 nm are $(1\,0\,\bar{1})$ and $(0\,1\,\bar{1})$ planes, respectively. These three groups of crystal planes form a nearly equal angle of *ca.* 120° with each other. It indicates that the exhibited facet is the (1 1 1) plane. The fast Fourier transform (FFT) pattern (Fig. 5e, inset) and the continuous lattice fringes observed at higher magnification (Fig. 5f) also verifies the well single crystalline nature of the tetragonal-rich $BaTiO_3$, from which few structure defects can be detected.

3.2. Ba^{2+} ions leaching behavior of the $BaTiO_3$ particles in aqueous medium

$BaTiO_3$ is not thermodynamically stable in aqueous solution because of the barium ions leaching behavior (shown in Eq. (1)), which actually is an important issue for the tape casting processing in electro-ceramic industry. Herein, the stability of $BaTiO_3$ in aqueous suspension is investigated from the point of the variation of phase structure for the first time. Hydrochloric acid (pH 2) is used as the medium because an acidic system is favor of Ba^{2+} ions leaching [25,27]. As shown in Table 1, the Ba^{2+} ions leached from the five samples are quite different. The Ba^{2+} ion concentration in the supernatant is gradually decreased with the increasing of synthetic temperature of the powders. As known, the leaching of Ba^{2+} ions in acidified water are carried out through the dissolution in a reactive surface layer of $BaTiO_3$ particles, and the thickness of reactive surface layer is inversely proportional to *S*/*V* (the ratio of total reactive surface area to solution volume) [27].

In the present study, 20 mg $BaTiO_3$ is dispersed in 1.25 mL dilute hydrochloric acid (pH 2). It is obvious that the suspension concentrations are same, but the amount of the Ba^{2+} ions leached differ greatly among the samples, for example, the Ba^{2+} ion concentration of the 120 °C-product is 3.6 times as large as those of samples obtained at 200 °C. The difference of the Ba^{2+} ions leaching ability is studied based on $BaTiO_3$ crystals

Table 1
The specific surface area and Ba/Ti atomic ratio of the products hydrothermally synthesized at different temperatures for 4 h and the corresponding Ba^{2+} ions concentration in the supernatant of their aqueous suspensions

	Synthetic temperature (°C)				
	120	140	160	180	200
Specific surface area (m^2/g)	29.8	25.5	22.2	18.5	17.0
Ba/Ti ratio	0.995	0.994	0.991	0.992	0.990
[Ba^{2+}] in supernatant (mg L^{-1})	1436	786.9	590.9	470.6	393.6

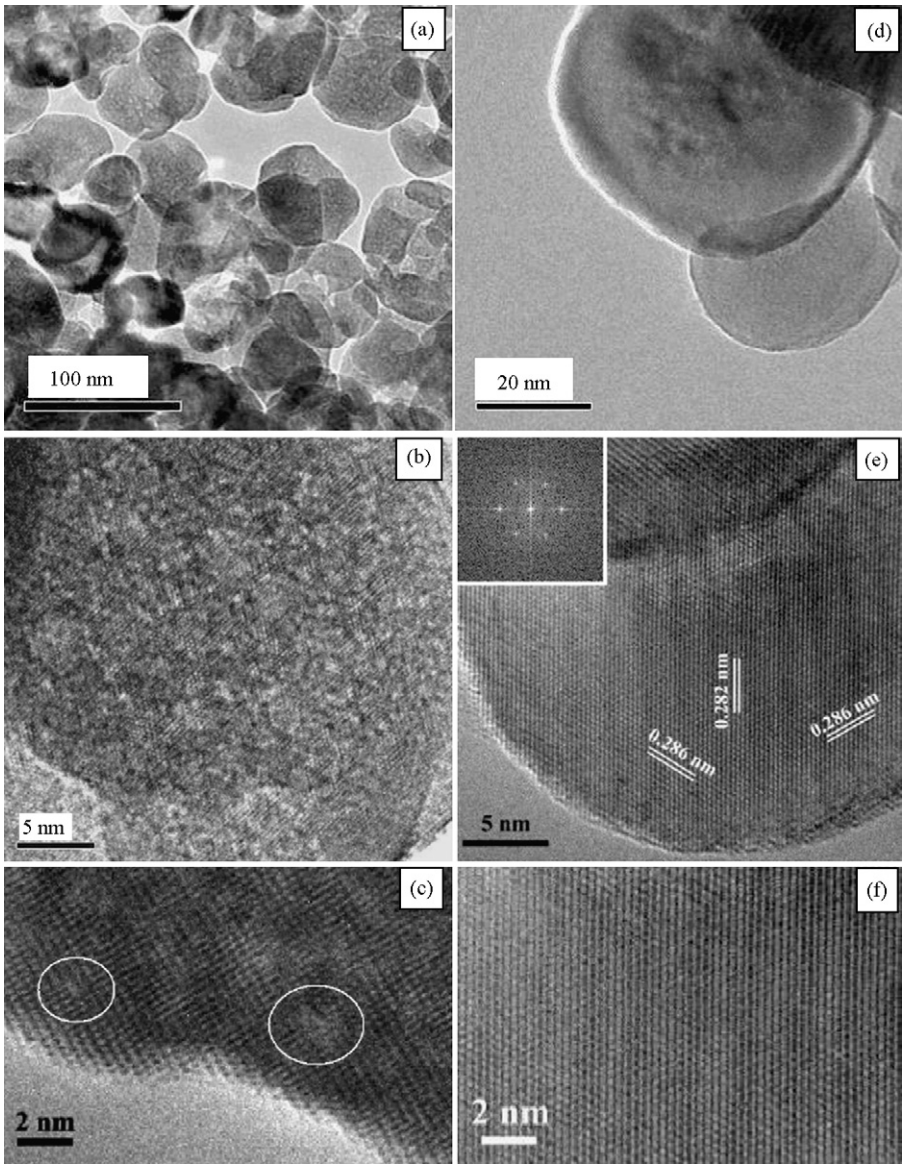

Fig. 5. TEM and HRTEM images of the hydrothermally synthesized $BaTiO_3$ particles at different reaction conditions: (a–c) 120 °C/1 h; (d–f) 200 °C/4 h. The inset of image (e) is the FFT pattern of the corresponding particle.

structure. Undoubtedly, the changing of the specific surface area (SSA) of $BaTiO_3$ particles will impact directly the *S*/*V* and subsequently affect the leached Ba^{2+} ions. According to the BET analysis (Table 1), the SSA of samples obtained decreases from 29.8 $m^2\ g^{-1}$ to 17.0 $m^2\ g^{-1}$ with the sample synthetic temperature increasing from 120 °C to 200 °C for a constant reaction time of 4 h. However, the difference in SSA cannot solely account for the variation of leached Ba^{2+} ions. This can be demonstrated by Fig. 6, in which the ratio of leached Ba^{2+} ions to SSA clearly decreases with the synthetic temperature increasing.

Ba/Ti atomic ratio of $BaTiO_3$ particles is also a factor that usually influences the Ba^{2+} ions leaching. Based on theoretical calculations, Jean et al. also revealed that the increasing of the leached Ba^{2+} concentration caused by the increase of the Ba/Ti ratio was occurred in a reactive surface layer of $BaTiO_3$ with a certain thickness rather than one layer of $BaTiO_3$ [26]. In the present experiment, the Ba/Ti ratio of the as-synthesized $BaTiO_3$ particles was measured. As shown in Table 1, the Ba/Ti ratios of the 4 h-products with different synthetic temperature varies from 0.995 to 0.990. Except for the 180 °C-product, the Ba/Ti ratio increases with the decreasing of the powders' synthetic temperature. However, this increase of Ba/Ti ratio cannot solely explain the difference of the Ba^{2+} ions leaching ability. In particular, the difference of the Ba/Ti ratio between the 120 °C-product and the 140 °C-product is only 0.001, however, the leached Ba^{2+} ions between these two samples differ most (shown in Fig. 6). Therefore, the Ba^{2+} ions leaching behavior of the presented $BaTiO_3$ particles is not influenced dominantly by the Ba/Ti ratio. The crystal structure transition should be considered.

TiO_6 octahedra in the perovskite-type $BaTiO_3$ have some distortion when the polymorph undergoes the transition from cubic to tetragonal. In typical $BaTiO_3$ structure, TiO_6 octahedra are conjoint by oxygen atoms on the vertex and the Ba atoms are filled within the 1×1 tunnels [37]. During the hydrother-

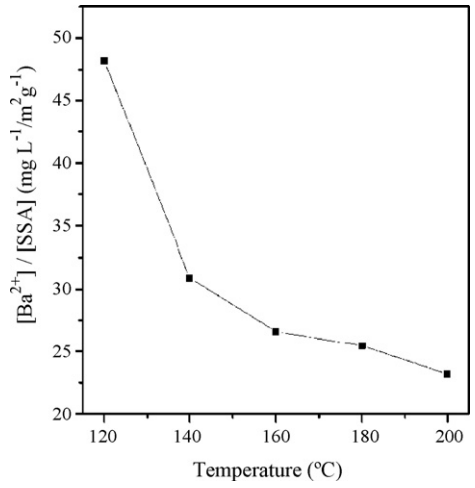

Fig. 6. The ratio of $[Ba^{2+}]$ in the supernatant to specific surface area (SSA) as a function of the synthetic temperature of 4 h-products.

mal process, the lattice constant a (and b) decreases when the reaction temperature increases from 120 °C to 200 °C. Consequently, it can be considered that the (0 0 1) planes have some shrinkage during the cubic-to-tetragonal transition. This shrinkage of a-axis and b-axis causes the tunnels along c direction to become more or less narrow, which, as a result, probably makes the diffusion of Ba^{2+} ions through the reactive surface layer in the aqueous suspension less easy compared with the non-shrinkage cubic samples. In addition, the large amounts of lattice defects existed in the cubic-rich samples also enhance the barium ions leaching ability due to their high reaction activity. This result is helpful for the electro-ceramic processing although more intensive study is necessary for this issue.

4. Conclusions

$BaTiO_3$ was hydrothermally synthesized at different reaction conditions, in which the continuous phase transition from cubic to tetragonal was found. A phase transition mechanism was proposed: the continuous phase transitions of $BaTiO_3$ during the hyrothermal synthesis are controlled by the competition between a kinetic-control process and a thermodynamic-control process, of which the former process favors the formation of cubic-rich $BaTiO_3$ whereas the latter is beneficial to the formation of tetragonal-rich structure. The barium ions leaching ability exhibited remarkable difference among the different $BaTiO_3$ aqueous suspensions because the crystal structures and the amount of the lattice defects vary continuously in the samples obtained at different hydrothermal conditions.

Acknowledgement

This work was supported by Doctoral Foundation in University of Jinan, P.R. China (XBS0706).

References

[1] Q. Feng, M. Hirasawa, K. Yanagisawa, Chem. Mater. 13 (2001) 290.
[2] Z.G. Shen, J.F. Chen, H.K. Zou, J. Yun, J. Colloid Interface Sci. 275 (2004) 158.
[3] A. Testino, M.T. Buscaglia, V. Buscaglia, M. Viviani, C. Bottino, P. Nanni, Chem. Mater. 16 (2004) 1536.
[4] M.C. Blanco-Lopez, B. Rand, F.L. Riley, J. Eur. Ceram. Soc. 17 (1997) 281.
[5] E. Brzozowski, M.S. Castro, J. Eur. Ceram. Soc. 20 (2000) 2347.
[6] J. Zeng, C. Lin, J. Li, K. Li, Mater. Lett. 38 (1999) 112.
[7] H. Matsuda, N. Kobayashi, T. Kobayashi, K. Miyazawa, M. Kuwabara, J. Non-Cryst. Solids 271 (2000) 162.
[8] K.M. Hung, W.D. Yang, C.C. Huang, J. Eur. Ceram. Soc. 23 (2003) 1901.
[9] P. Duran, F. Capel, D. Gutierrez, J. Tartaj, M.A. Banares, C. Moure, J. Mater. Chem. 11 (2001) 1828.
[10] Y. Ma, E. Vileno, S.L. Suib, P.K. Dutta, Chem. Mater. 9 (1997) 3023.
[11] Y. Hakuta, H. Ura, H. Hayashi, K. Arai, Ind. Eng. Chem. Res. 44 (2005) 840.
[12] A. Testino, V. Buscaglia, M.T. Buscaglia, M. Viviani, P. Nann, Chem. Mater. 17 (2005) 5346.
[13] R.I. Walton, F. Millange, R.I. Smith, T.C. Hansen, D. O'Hare, J. Am. Chem. Soc. 123 (2001) 12547.
[14] P.K. Dutta, J.R. Gregg, Chem. Mater. 4 (1992) 843.
[15] P.K. Dutta, R. Asiaie, S.A. Akbar, W. Zhu, Chem. Mater. 6 (1994) 1542.
[16] R. Asiaie, W. Zhu, S.A. Akbar, P.K. Dutta, Chem. Mater. 8 (1996) 226.
[17] S.K. Tripathy, T. Sahoo, M. Mohapatra, S. Anand, R.P. Das, Mater. Lett. 59 (2005) 3543.
[18] S.K. Lee, T.J. Park, G.J. Choi, K.K. Koo, S.W. Kim, Mater. Chem. Phys. 82 (2003) 742.
[19] C.D. Chandler, C. Roger, M.J. Hampden-Smith, Chem. Rev. 93 (1993) 1205.
[20] G. Busca, V. Buscaglia, M. Leoni, P. Nannit, Chem. Mater. 6 (1994) 955.
[21] L.A. Pérez-Maqueda, M.J. Diánez, F.J. Gotor, M.J. Sayagués, C. Real, J.M. Criado, J. Mater. Chem. 13 (2003) 2234.
[22] S.W. Lu, B.I. Lee, Z.L. Wang, W.D. Samuels, J. Cryst. Growth 219 (2000) 269.
[23] I.J. Clark, T. Takeuchi, N. Ohtoric, D.C. Sinclaira, J. Mater. Chem. 9 (1999) 83.
[24] B.D. Begg, E.R. Vance, J. Nowotny, J. Am. Ceram. Soc. 77 (1994) 3186.
[25] A. Neubrand, R. Lindner, P. Hoffmann, J. Am. Ceram. Soc. 83 (2000) 860.
[26] C.W. Chiang, J.H. Jean, Mater. Chem. Phys. 80 (2003) 647.
[27] U. Paik, V.A. Hackley, J. Am. Ceram. Soc. 83 (2000) 2381.
[28] H.W. Nesbitt, G.M. Bancroft, W.S. Fyfe, S.N. Karkhanis, A. Nishijima, S. Shin, Nature 289 (1981) 358.
[29] U. Paik, S. Lee, V.A. Hackley, J. Am. Ceram. Soc. 86 (2003) 1662.
[30] M.C. Blanco-López, B. Rand, F.L. Riley, J. Eur. Ceram. Soc. 20 (2000) 1587.
[31] Z.C. Chen, T.A. Ring, J. Lemaitre, J. Am. Ceram. Soc. 75 (1992) 3201.
[32] J.H. Jean, H.R. Wang, J. Am. Ceram. Soc. 81 (1998) 1589.
[33] J.H. Jean, H.R. Wang, J. Am. Ceram. Soc. 83 (2000) 277.
[34] B.D. Begg, K.S. Finnie, E.R. Vance, J. Am. Ceram. Soc. 79 (1996) 2666.
[35] E.W. Shi, C.T. Xia, W.E. Zhong, B.G. Wang, C.D. Feng, J. Am. Ceram. Soc. 80 (1997) 1567.
[36] R. Viekanandan, T.R.N. Kutty, Powder Technol. 57 (1989) 181.
[37] A. Clearfield, Chem. Rev. 88 (1988) 125.